

Machine learning for predictive condensed-phase simulation

Albert P. Bartók*, Michael J. Gillan†, Frederick R. Manby‡
Gábor Csányi*

January 17, 2021

Abstract

We show how machine learning techniques based on Bayesian inference can be used to reach new levels of realism in the computer simulation of molecular materials, focusing here on water. We train our machine-learning algorithm using accurate, correlated quantum chemistry, and predict energies and forces in molecular aggregates ranging from clusters to solid and liquid phases. The widely used electronic-structure methods based on density-functional theory (DFT) give poor accuracy for molecular materials like water, and we show how our techniques can be used to generate systematically improvable corrections to DFT. The resulting corrected DFT scheme gives remarkably accurate predictions for the relative energies of small water clusters and of different ice structures, and greatly improves the description of the structure and dynamics of liquid water.

1 Introduction

The computer simulation of materials has become an indispensable tool across a wide range of disciplines, including chemistry, metallurgy, the earth sciences, surface science and biology. Simulation techniques range all the way from simple empirical force fields to the electronic structure methods based on density functional theory (DFT) and correlated quantum chemistry [1]. Electronic structure methods are capable of much greater accuracy and generality than force fields, but their computational demands are heavier by many orders of magnitude. A

*Engineering Laboratory, University of Cambridge, Trumpington Street, Cambridge, CB2 1PZ, United Kingdom

†London Centre for Nanotechnology, University College London, Gordon St., London WC1H 0AH, United Kingdom; Department of Physics and Astronomy, University College London, Gower St., London WC1E 6BT, United Kingdom; Thomas Young Centre, University College London, Gordon St., London WC1H 0AH, United Kingdom

‡Centre for Computational Chemistry, School of Chemistry, University of Bristol, Bristol BS8 1TS, United Kingdom

crucial challenge for simulation is therefore to find systematically improvable methods for casting information from accurate electronic-structure techniques into forms that are more rapidly computable. We show here how machine learning techniques [2] allow this to be done using correlated quantum chemistry for molecular materials, taking condensed-phase water as our example.

The fundamental interactions in water and other molecular materials [3] consist of exchange-repulsion, electrostatic interaction between molecular charge distributions, polarization (i.e. the electrostatic distortion of charge distributions), charge transfer and van der Waals dispersion, together with effects due to molecular flexibility. Electron correlation plays a role in all these, and is crucial for dispersion [4]. The correlated quantum chemistry methods of MP2 (2nd-order Møller-Plesset) and particularly CCSD(T) (coupled-cluster with single and double excitations and perturbative triples) [5] give a very accurate description of these interactions [6, 7], but their heavy computational demands for extended systems make their routine use for condensed matter problematic. DFT techniques are less demanding, and have been widely used for water [8], but it has been found that the results with standard approximations often agree poorly with experiment [9] and may depend strongly on the assumed approximation [10]. There is vigorous debate about how to overcome the problems, and we believe that input from correlated quantum chemistry is essential. In the approach described here, machine learning [2] is used to construct representations of the energy differences between correlated quantum chemistry and DFT, which can then be used to construct efficient corrected DFT schemes for simulation of large, complex systems.

Our machine-learning methods are based on the recently reported ideas of Gaussian Approximation Potentials (GAP) [11, 12]. For molecular materials, we use these ideas in the framework of the widely used many-body representation [13, 14], in which the total energy $E_{\text{tot}}(1, 2, \dots, N)$ of a system of N molecules is separated into 1-body, 2-body and beyond-2-body parts:

$$E_{\text{tot}}(1, \dots, N) = \sum_{i=1}^N E_{1\text{B}}(i) + \sum_{i < j} E_{2\text{B}}(i, j) + E_{\text{B2B}}(1, \dots, N). \quad (1)$$

Here, $E_{1\text{B}}(i)$ is the 1-body energy of molecule i in free space, which depends on its distortion away from its equilibrium configuration. The energy $E_{2\text{B}}(i, j)$ is the 2-body interaction energy of the pair of molecules (i, j) in free space, i.e. the total energy of the pair minus the sum of their 1-body energies. For water, $E_{2\text{B}}(i, j)$ is a function of 12 variables specifying the separation of the molecules, their relative orientation and their internal distortions. The beyond-2-body (B2B) energy E_{B2B} represents everything not accounted for by 1- and 2-body energies. Exchange-repulsion, 1st-order electrostatics and dispersion are mainly or entirely 2-body interactions, while E_{B2B} arises mainly from polarization and perhaps charge transfer, with contributions from exchange-repulsion and dispersion expected to be smaller [15]. The ideas in the present paper build on the pioneering works in the groups of Szalewicz [16] and Bowman [17].

The energy of an isolated H_2O monomer as a function of distortion is known

from *ab initio* calculations to extremely high precision. We use the parameterization due to Partridge and Schwenke (PS) [18], which can be regarded as essentially exact for our purposes. In water and many other molecular materials, the 2-body interactions give the largest contribution to the binding energy, so these must be accurately represented [19]. However, in water, the B2B interactions also play a crucial role [16]. It has long been known that there is a strong redistribution of electrons when a water monomer enters the liquid or solid phases, and its dipole moment increases from 1.8 D in the gas phase to ~ 2.5 D or more in condensed phases [20]. The B2B terms in the energy come partly from the large changes of electrostatic interactions due to this redistribution. In the strategy presented here, the B2B part of the energy is represented by a chosen form of DFT, because DFT can be expected to include most of the physical effects that play a role in the B2B energy. We will discuss at the end how such an approximation to B2B interactions can be further improved. We note here that we fully include molecular flexibility, which is not always done even in sophisticated empirical interaction models. Flexibility is essential, because without it one could not describe the well known lengthening of O-H bonds and the lowering of O-H vibrational frequency [21] when the H atom participates in a hydrogen bond with another monomer, and nor could quantum nuclear effects [22] be properly treated.

2 Machine learning with GAP

Consider a system whose configuration is specified by points \mathbf{R} in a many-dimensional configuration space. We are given the values $f(\mathbf{R}_n)$ of its energy at a finite set of configurations $\{\mathbf{R}_n\}$. We now ask: what is the most likely value of $f(\mathbf{R})$ at a configuration \mathbf{R} not in the given set $\{\mathbf{R}_n\}$? The rules of Bayesian inference [2] are used to compute this most likely value, assuming that the function f has certain smoothness properties. Here smoothness simply means that the probability of finding very different values $f(\mathbf{R})$ and $f(\mathbf{R}')$ decreases rapidly to zero as \mathbf{R} and \mathbf{R}' approach each other. The framework of GAP, based on Gaussian processes [23], uses a precise formulation of smoothness in terms of a covariance function $C(\mathbf{R}, \mathbf{R}')$ having the form [23]:

$$C(\mathbf{R}, \mathbf{R}') = \theta \exp \left(- \sum_i [(R_i - R'_i)/(2\sigma_i)]^2 \right), \quad (2)$$

where the sum in the exponent is over the dimensions of the configuration space, θ is the typical scale of f and σ is the typical length scale on which $f(\mathbf{R})$ varies. The theory yields the following formula [23] for the most likely estimate of $f(\mathbf{R})$ given the data and the assumption of smoothness (often called the maximum *a posteriori* estimator):

$$f(\mathbf{R}) = \sum_n^{\text{data}} C(\mathbf{R}, \mathbf{R}_n) \alpha_n, \quad (3)$$

where the coefficients α_n are given by inversion of the linear equations:

$$f(\mathbf{R}_m) = \sum_n^{\text{data}} [C(\mathbf{R}_m, \mathbf{R}_n) + \varepsilon \delta_{mn}] \alpha_n, \quad (4)$$

where δ_{mn} is the Kronecker delta; the diagonal shift of magnitude ε is included to regularise the linear algebra.

When applying GAP to represent 1- and 2-body energetics in water, there are different ways of choosing the space of points \mathbf{R} representing configurations, but here it is advantageous to build in the fact that the energy function $f(\mathbf{R})$ is left unchanged by rotations and translations of the whole system, and by interchange of identical atoms. For the water monomer, the two OH distances and the angle between them provide a convenient coordinate system. For the water dimer, we ensure rotation and translation symmetry by working with the space of the 15 interatomic distances, $\mathbf{R} = \{|\mathbf{r}_i - \mathbf{r}_j|\}$, where \mathbf{r}_i are the atomic positions. To ensure interchange symmetry, we symmetrize the covariance function over permutations of identical atoms:

$$\tilde{C}(\mathbf{R}, \mathbf{R}') = \frac{1}{|S|} \sum_{\pi \in S} C(\pi(\mathbf{R}), \mathbf{R}'), \quad (5)$$

where S is the permutation group of the water dimer, whose order $|S|$ is 8. A more detailed account of our GAP formalism is given in [11] and [12]. The computational cost of evaluating the GAP model is linear in the size of the database $\{\mathbf{R}_n\}$, and for the present case takes about 10 ms on a single processor.

Recently, Gaussian processes were used to model the atomisation energies of small molecules[24], and a similar technique (based on neural networks) was used to fit the total energy of the water dimer in the DFT approximation [25]. Rather than using GAP to represent the whole dimer energy, we use it to represent the difference between basis-set converged CCSD(T) and DFT, in other words the DFT error. In practice, we do this in two stages. In the first stage, we compute the difference between MP2 and DFT at about ten thousand dimer configurations, using the AVTZ basis. In using GAP to represent this difference, we also use the gradients of the potential energy surface (see SI). In the second stage, we construct a GAP model using around one thousand energies (without forces) to represent the small difference between MP2/AVTZ and CCSD(T), the latter converged with respect to the basis set to about 1 meV.

In the calculations to be presented, we use GAP to correct the popular Becke-Lee-Yang-Parr (BLYP) approximation of DFT, our choice being guided by the fact that BLYP is accurate for the B2B energy of small water clusters (see SI). We show in Fig. 1 the 2-body errors of BLYP together with the errors of GAP-corrected BLYP for a thermal sample of dimer configurations (which were not used in the construction the GAP model) drawn from a molecular dynamics simulation of liquid water. Uncorrected BLYP is too repulsive for the water dimer, with unacceptably large errors of up to 50 meV at the separations of interest. However, with GAP corrections, the errors are dramatically reduced

to ~ 1 meV. GAP thus provides a way of virtually eliminating all errors in a chosen DFT approximation apart from those associated with B2B energy. Also shown in Fig. 1 are the errors of the approximation obtained by the popular procedure of adding the dispersion correction due to Grimme *et al.* [26] to BLYP. We note that this approximation is better than uncorrected BLYP, but is much less good than GAP-corrected BLYP.

3 Results

To illustrate the power of our GAP-corrected DFT, we start with a simple test on the ten stationary points of the water dimer [27]. These form a canonical set of configurations, which have been exhaustively studied and whose energies are extremely accurately known [6]. The global minimum structure is bound by a single hydrogen bond, but some of the less stable structures have up to four weaker hydrogen bonds. (For pictures of the structures, see e.g. Ref. [6].) We stress that none of these stationary points is included in our training set, so that the energies computed with BLYP + GAP are genuine predictions. We compare in Table 1 the relative energies of the 10 configurations from BLYP + GAP with the almost exact results from Ref. [6] and the predictions of the DFT functional BLYP; the Table also includes the very accurate predictions of diffusion Monte Carlo (DMC) [28]. As has been reported before [29], the DFT approximation shows quite large errors of around 30 meV in some cases, while the errors of DMC are much smaller, being almost all less than 3 meV. Our BLYP + GAP predictions are very accurate, and indeed they compete in accuracy with DMC, at enormously reduced computational cost.

As a second test, we examine the predictions of BLYP+GAP for the energies of different isomers of the water hexamer. This system has been studied extensively for many years [14, 30, 7], for a very important reason. The most stable structures of small water clusters from the trimer to the pentamer have a ring-like form in which each monomer is hydrogen bonded to two neighbours [30]. However, from the hexamer onwards, rings are less stable than compact structures in which some monomers are hydrogen bonded to three or four neighbours [30, 31, 7]. The energy balance for the hexamer is rather delicate, but high-precision CCSD(T) calculations leave no doubt that the compact prism and cage structures have lower energy than the more open book and ring forms [7]. However, many of the commonly used DFT approximations, including BLYP and PBE, wrongly predict that the ring or book form is most stable [32]. We compare in Figure 2 the predictions of BLYP + GAP with CCSD(T) benchmarks and with the predictions of BLYP and DMC. We see that again the GAP-corrected DFT model is highly accurate and is comparable to DMC.

For any material, crystal energetics provides a crucial test of modelling techniques. Water has a remarkably rich phase diagram, with no fewer than fifteen known ice structures [33, 34]. In the common form ice Ih, found at ambient pressure, each H_2O monomer is H-bonded to four nearest neighbours at an O-O distance of 2.75 Å, the next-nearest neighbours having the much greater O-O

separation of 4.5 Å. The pattern of H-bonding in ice Ih is disordered, but the closely related ordered form ice XI, stable below 72 K, has essentially the same local geometry [33]. With increasing pressure, denser structures become more stable, and we will be concerned here with (in order of increasing density) ice IX, II, XV and VIII. The distances to non-H-bonded next-nearest neighbours decrease along this series, becoming almost exactly equal to the first-neighbour distance in ice VIII [33]. There are accurate experimental values for the zero-pressure energies and volumes of almost all these structures.

Standard DFT approximations perform poorly for ice [35], making the energies increase far too much from ice Ih to VIII, and giving transition pressures too high by up to a factor of 10. Our machine-learning techniques allow us to correct any DFT approximation for 1- and 2-body errors, and enable us to discover whether these errors are responsible for the poor description of ice energetics. We have used BLYP + GAP to calculate the relaxed geometries and the equilibrium energies and volumes of the ice structures mentioned above, substituting the periodic Bernal and Fowler structure for the proton-disordered Ih [36]. The results are reported in Table 2, where we also give results obtained with uncorrected BLYP. The energies and volumes relative to ice Ih are very accurately given by BLYP + GAP, whereas the relative energies with uncorrected BLYP suffer the large errors reported earlier for standard DFT methods [35]. However, our results also reveal a significant *uniform* overbinding in all the structures due to beyond-2-body errors, implying that BLYP + GAP overestimates the strength of cooperative H-bonding, leading to an overestimate of the equilibrium density by about 5–10%. The systematic overestimation of density by BLYP + GAP would be partially compensated by zero-point effects, which increase volumes by between 1–5% [37].

Early attempts to elucidate the properties of liquid water on the molecular level using DFT were promising [8], but it has turned out that the standard methods give surprisingly poor predictions [9], for reasons that are presumably linked to the problems found with ice structures. Other molecular liquids seem to suffer from related difficulties [38]. Some of the common approximate functionals give an equilibrium density of water that is too low by as much as 30% (PBE and BLYP underestimate it by ~10% and 10–20% respectively) [10, 39]. In DFT simulations of the liquid at the experimental density, the diffusion coefficient may be too low by as much as a factor of 10, and the liquid is significantly overstructured [10] as compared with experimental neutron and x-ray diffraction data. Quite apart from the contradictions with experiment, it is now clear that the DFT simulations may be afflicted by many technical sources of error, including system size effects, basis-set incompleteness, incorrect temperature control, and the neglect of quantum nuclear effects. Because of the controversies, we approach the liquid with caution, particularly since our machine-learning methods for going beyond DFT do not yet account for errors in B2B interactions. Nevertheless, we can address an important and well defined question: With machine-learning used to ensure the correctness of 1B and 2B parts of the energy, can DFT errors in the B2B energies still cause contradictions with experiment?

We performed molecular dynamics simulations on 64 molecules of liquid heavy water (D_2O) with BLYP + GAP at temperature 308 K and density 1.109 g cm^{-3} . The thermal average pressure in the simulation was -2.6 kbar . By contrast, a simulation based on BLYP itself under exactly the same conditions gives the larger pressure of 7 kbar , which is associated with the 10–20% underestimate of equilibrium density. A simple estimate based on our observed pressure together with the experimental compressibility indicates that the equilibrium density with BLYP + GAP is higher than the correct value by $\sim 10\%$, which is consistent with the uniform overbinding observed above for the ice structures.

We compute the self-diffusion coefficient D of molecules in our simulation in the conventional way [40] from the slope of the time-dependent mean-square displacement (for details, see SI), finding the value $1.3 \times 10^{-9} \text{ m}^2 \text{ s}^{-1}$. In a system of only 64 molecules, the value of D is expected to be reduced by size effects by an amount that can be estimated by standard methods [41]. Our size-corrected value (see SI) of $1.7 \times 10^{-9} \text{ m}^2 \text{ s}^{-1}$ should be compared with the experimental value of $2.4 \times 10^{-9} \text{ m}^2 \text{ s}^{-1}$ [42]. This contrasts with the values reported for BLYP itself, which are up to an order magnitude too small [10, 43, 44]. Once again, 2-body effects appear to be the main culprit in making BLYP unrealistic.

The well known DFT errors of overstructuring in liquid water are most clearly seen in the oxygen-oxygen radial distribution function $g_{\text{OO}}(r)$. A comparison of the experimental and computed RDFs (using BLYP + GAP and uncorrected BLYP — see Fig. 3) shows that the GAP correction very significantly improves agreement with experiment. The overstructuring of the liquid is largely corrected: the first peak in $g_{\text{OO}}(r)$ is lowered by ~ 0.25 and the first trough becomes shallower by ~ 0.2 . However, our comparison with experimental data indicates that the liquid is probably still slightly overstructured even with BLYP + GAP. We have chosen to compare here with a joint refinement of both neutron and x-ray data [45], but one should note the extensive discussion in the literature about the uncertainties in both kinds of experimental data. We attempt to give a balanced summary of this discussion in the SI. In addition, since our simulation treats the nuclei as classical particles, it is essential to consider quantum nuclear corrections. Our discussion of the experimental and theoretical evidence about these (see SI) indicates that they may lower the first peak height of $g_{\text{OO}}(r)$ by ~ 0.1 . Our assessment that water simulated with BLYP + GAP is slightly overstructured takes account of both the experimental uncertainties and the quantum nuclear effects.

4 Discussion and conclusions

The machine-learning methods we have described offer a new approach to the modelling of molecular materials. To show the possibilities, we have discussed only a single material (water) and we have focused on the systematic improvement of the 1- and 2-body parts of the energy. Furthermore, the use of machine

learning to represent the difference between DFT and accurate quantum chemistry (and thus incurring the cost of DFT when running a simulation) is only one of several possible strategies. There is ample scope for removing these limitations in the future. Note, however, what has already been achieved even with these limitations. The description of water energetics for aggregation states ranging from clusters to extended solid and liquid states is challenging because of the delicate balance between different components of the energy. We have shown how to use machine learning to construct a quantitative correction for 1-, 2-body components of the energy, starting from a chosen DFT approximation (in this case, BLYP). We have achieved a substantial improvement in the description of cluster and ice-phase energetics and liquid-state properties, with a completely negligible increase in computational cost, and we have also revealed a remaining inaccuracy in the beyond-2-body energetics, which we attribute to exaggerated cooperativity of H-bonding.

The most obvious generalisation now needed is to use machine learning to systematically improve the beyond-2-body energetics. In fact, GAP-based machine learning has already been used with great success to represent many-body energies in other types of systems [12], and there is every reason to expect that this can be done for molecular systems. As a first step, we plan to use accurate beyond-2-body energies generated for large samples of configurations of small and moderate sized clusters, as we have already done in a recent paper [28]. Benchmark information from quantum Monte Carlo for configuration samples of larger clusters and for the liquid may also be helpful.

Our strategy of using GAP to represent corrections to be added to DFT is powerful in terms of generality, but large gains in computational efficiency could be achieved with other strategies. The use of GAP to represent corrections to empirical force fields, particularly those that already account for molecular flexibility and for many-body effects (see e.g. Ref. [46, 47, 48]), holds much promise for the future. However, we note that although such models already exist for water, as a result of many years of development effort, the same is true of very few other molecular systems.

We have focused here on water, because of its outstanding importance for science and society, but the present methods should be readily applicable to many other molecular systems, even without the technical improvements we have mentioned. The cluster, solid and liquid states of simple molecules such as ammonia and hydrogen fluoride are obvious targets, but many kinds of mixture, including the environmentally and industrially important gas hydrates, are also accessible.

5 Materials and Methods

All calculations on molecules and isolated molecular assemblies were carried out using the Molpro package[50]. The water dimer configurations were obtained from a long equilibrium simulation of liquid water using the AMOEBA force field[51].

We used the Castep code [52] for the DFT calculations on ice structures, and

a modified version of the VASP code [53] for the molecular dynamics simulations of liquid heavy water (D_2O). Here, the number of molecules per unit volume is the same as for H_2O at 0.997 g cm^{-3} . Further technical details about basis-set completeness, time-step, temperature control etc are given in the Supplementary Information (SI), but we note that thermal averages were computed on a run of 45 ps duration of which 20 ps was discarded for equilibration.

Software and data are available at <http://www.libatoms.org>.

6 Acknowledgements

ABP was supported by a Junior Research Fellowship at Magdalene College, Cambridge. GC acknowledges supported from the Office of Naval Research under grant number N000141010826, and EU-FP7-NMP grant 229205 ADGLASS. The authors are grateful to D O'Neill for his important contribution to an earlier incarnation of this project, and FRM gratefully acknowledges funding from the Engineering and Physical Sciences Research Council (EP/F000219/1). The authors thank AK Soper and CJ Benmore for useful discussions.

References

- [1] Sydney Yip (ed.) (2005) Handbook of Materials Modeling, (Springer, Dordrecht)
- [2] David J. C. Mackay (2005) Information Theory, Inference and Learning Algorithms (Cambridge University Press, Cambridge)
- [3] Stone AJ (1996) The Theory of Intermolecular Forces (Oxford University Press, Oxford).
- [4] Klimeš J, Michaelides A (2012) Perspective: Advances and challenges in treating van der Waals dispersion forces in density functional theory. *J Chem Phys* 137: 120901.
- [5] Helgaker T, Jorgensen P, Olsen J (2000) *Molecular Electronic-Structure Theory* (Wiley, New York).
- [6] Tschumper GS *et al.* (2002) Anchoring the water dimer potential energy surface with explicitly correlated computations and focal point analysis. *J Chem Phys* 116: 690.
- [7] Bates DM, Tschumper GS (2009) CCSD(T) complete basis set limit relative energies for low-lying water hexamer structures. *J Phys Chem A* 113: 3555.
- [8] Laasonen K, Sprik M, Parrinello M, Car R (1993) “Ab initio” liquid water. *J Chem Phys* 99: 9080.

- [9] Grossman JG, Schwegler E, Draeger EW, Gygi F, Galli G (2004) Towards an assessment of the accuracy of density functional theory for first-principles simulations of water. *J Chem Phys* 120: 300.
- [10] Wang J, Román-Pérez, Soler JM, Artacho E, Fernández-Serra (2011) Density, structure and dynamics of water: The effect of van der Waals interactions *J Chem Phys* 134: 024516.
- [11] Bartók AP (2009), Gaussian Approximation Potential: an interatomic potential derived from first principles quantum mechanics, *PhD Thesis*, University of Cambridge, also available at <http://arxiv.org/abs/0910.1019>
- [12] Bartók A, Payne MC, Kondor R, Csányi G (2010) Gaussian approximation potentials: the accuracy of quantum mechanics, without the electrons. *Phys Rev Lett* 104:136403.
- [13] Xantheas SS (1994) Ab initio studies of cyclic water clusters $(\text{H}_2\text{O})_n$, $n = 1 - 6$. II. Analysis of many-body interactions. *J Chem Phys* 110: 7523-7534.
- [14] Pedulla JM, Vila F, Jordan KD (1996) Binding energy of the ring form of $(\text{H}_2\text{O})_6$: Comparison of the predictions of conventional and localized-orbital MP2 calculations. *J Chem Phys* 105: 11091.
- [15] Wang F-F, Jenness G, Al-Saidi WA, Jordan KD (2010) Assessment of the performance of common density functional methods for describing the interaction energies of $(\text{H}_2\text{O})_6$ clusters. *J Chem Phys* 132: 134303.
- [16] Bukowski B, Szalewicz K, Groenenboom GC, van der Avoird A (2007) Prediction of the properties of water from first principles. *Science* 315: 1249-1252.
- [17] Wang, Y., Huang, X., Shepler, B. C., Braams, B. J., and Bowman, J. M. (2011). Flexible, ab initio potential, and dipole moment surfaces for water. I. Tests and applications for clusters up to the 22-mer. *J Chem Phys* 134: 094509.
- [18] Partridge H, Schwenke DW (1997) The determination of an accurate isotope dependent potential energy surface for water from extensive ab initio calculations and experimental data. *J Chem Phys* 106: 4618.
- [19] Hodges MP, Stone AJ, Xantheas SS (1997) Contribution of many-body terms to the energy for small water clusters: A comparison of ab initio calculations and accurate model potentials. *J Phys Chem A* 101: 9163.
- [20] Coulson CA, Eisenberg D (1966) Interactions of H_2O molecules in ice: I. The dipole moment of an H_2O molecule in ice. *Proc R Soc London Ser A* 291: 454.
- [21] Jeffrey GA (1997) *An Introduction to Hydrogen Bonding* (Oxford University Press, Oxford), ch. 11.

- [22] Habershon S, Markland TE, Manolopoulos DE (2009) Computing quantum effects in the dynamics of a flexible water model. *J Chem Phys* 131: 024501.
- [23] C. E. Rasmussen and C. K. I. Williams (2006) Gaussian Processes for Machine Learning (The MIT Press, Boston)
- [24] Rupp, M., Tkatchenko, A., Müller, K.-R., and Lilienfeld, von, O. (2012). Fast and Accurate Modeling of Molecular Atomization Energies with Machine Learning. *Phys Rev Letts* 108(5): 058301
- [25] Morawietz, T., Sharma, V., and Behler, J. (2012). A neural network potential-energy surface for the water dimer based on environment-dependent atomic energies and charges. *J Chem Phys* 136(6): 064103.
- [26] Grimme S, Antony J, Ehrlich S, Krieg H (2010) DFT-D3: A dispersion correction for DFT functionals. *J Chem Phys* 132: 154104.
- [27] Smith BJ, Swanton DJ, Pople JA, Schaefer HF, Radon L (1990) Transition structures for the interchange of hydrogen atoms within the water dimer. *J Chem Phys* 92: 1240.
- [28] Gillan MJ, Manby FR, Towler MD, Alfè D (2012) Assessing the accuracy of quantum Monte Carlo and density functional theory for energetics of small water clusters. *J Chem Phys* 136: 244105.
- [29] Anderson JA, Tschumper GS (2006) Characterizing the potential energy surface of the water dimer with DFT: Failures of some popular functionals for hydrogen bonding. *J Phys Chem A* 110: 7268.
- [30] Gregory JK, Clary DC, Liu K, Brown MG, Saykally RJ (1997) The water dipole moment in water clusters. *Science* 275: 814.
- [31] Kim J, Majumdar D, Lee HM, Kim KS (1999) Structures and energetics of the water heptamer: Comparison with the water hexamer and octamer. *J Chem Phys* 110: 9128.
- [32] Santra B *et al.* (2008) On the accuracy of density-functional theory exchange-correlation functionals for H bonds in small water clusters. II. The water hexamer and van der Waals interactions. *J Chem Phys* 129: 194111.
- [33] Petrenko V, Whitworth RW (1999) *Physics of Ice* (Oxford University Press, Oxford).
- [34] Salzmann CG, Radaelli PG, Mayer E, Finney JL (2009) Ice XV: A new thermodynamically stable phase of ice. *Phys Rev Lett* 103: 105701.
- [35] Santra *et al.* (2011) Hydrogen bonds and van der Waals forces in ice at ambient and high pressures. *Phys Rev Lett* 107: 185701.

- [36] Bernal JD, and Fowler RH (1933). A theory of water and ionic solution, with particular reference to hydrogen and hydroxyl ions. *J Chem Phys* 1(8): 515-548.
- [37] Murray É and Galli, G (2012). Dispersion interactions and vibrational effects in ice as a function of pressure: a first principles study. *Phys. Rev. Lett.* 108: 105502.
- [38] McGrath MJ, Kuo IFW, Siepmann JI (2011) Liquid structures of water, methanol and hydrogen fluoride at ambient conditions from first-principles molecular dynamics simulations with a dispersion corrected density functional. *Phys Chem Chem Phys* 13: 19943.
- [39] Ma, Z., Zhang, Y., and Tuckerman, M. E. (2012). Ab initio molecular dynamics study of water at constant pressure using converged basis sets and empirical dispersion corrections. *J Chem Phys* 137: 044506.
- [40] Frenkel D, Smit B (2002) *Understanding Molecular Simulation* (Academic Press, SanDiego).
- [41] Dünweg B, Kremer K (1993) Molecular dynamics simulation of a polymer chain in solution. *J Chem Phys* 99: 6983-6997.
- [42] Hardy EH, Zygar A, Zeidler MD, Holz M, Sacher FD (2001) Isotope effect on the translational and rotational motion in liquid water and ammonia. *J Chem Phys* 114: 3174.
- [43] Jonchiere, R., Seitsonen, A. P., Ferlat, G., Saitta, A. M., and Vuilleumier, R. (2011). Van der Waals effects in ab initio water at ambient and super-critical conditions. *J Chem Phys* 135(15): 154503.
- [44] Lee, H.-S., and Tuckerman, M. E. (2007). Dynamical properties of liquid water from ab initio molecular dynamics performed in the complete basis set limit. *J Chem Phys* 126(16): 164501.
- [45] Soper AK (2007) Joint structure refinement of x-ray and neutron diffraction data on disordered materials: application to liquid water. *J Phys Condens Matter* 19: 335206.
- [46] Fanourgakis GS, Xantheas SS (2008) Development of transferable interaction potentials for water. V. Extension of the flexible, polarizable, Thole-type model potential to describe the vibrational spectra of water clusters and liquid water. *J Chem Phys* 128: 074506.
- [47] Hasegawa T, Tanimura Y (2011) A polarizable water model for intramolecular and intermolecular vibrational spectroscopies. *J Phys Chem B* 115: 5545.
- [48] Babin V, Medders GR, Paesani F (2012) Toward a universal water model: First principles simulations from the dimer to the liquid phase. *J Phys Chem Lett* 3: 3765.

Table 1: Relative energies of the 10 stationary points of the water dimer computed with CCSD(T) close to the basis-set limit [6], diffusion Monte Carlo [28], DFT with the BLYP functional and BLYP+GAP. Numbering of the stationary states is standard (see e.g. Ref. [6]). Units: meV.

State	BLYP	BLYP+GAP	CCSD(T)	DMC
1	0	0	0	0
2	23	23	21	24
3	32	27	25	27
4	49	32	30	34
5	65	44	41	39
6	73	45	44	41
7	96	79	79	78
8	155	153	154	156
9	95	82	77	79
10	125	116	117	122

- [49] Whalley E (1984) Energies of the phases of ice at zero temperature and pressure. *J Chem Phys* 81: 4087.
- [50] Werner H-J, Knowles PJ, Knizia G, Manby FR and Schütz M (2012). Molpro: a general-purpose quantum chemistry program package. *WIREs Comput Mol Sci* 2: 242-253; Werner H-J *et al.* (2012) MOLPRO, version 2012.1, a package of ab initio programs, Cardiff, UK. <http://www.molpro.net>
- [51] Ren P, Ponder JW (2003) Polarizable atomic multipole water model for molecular mechanics simulation. *J Phys Chem B* 107: 5933.
- [52] Clark SJ, Segall MD, Pickard CJ, Hasnip PJ, Probert MJ, Refson K and Payne MC (2005) First principles methods using CASTEP. *Z Krist* 220: 567-570
- [53] Kresse G and Furthmüller J (1996). Efficiency of ab-initio total energy calculations for metals and semiconductors using a plane-wave basis set. *Comput. Mat. Sci.* 6: 15

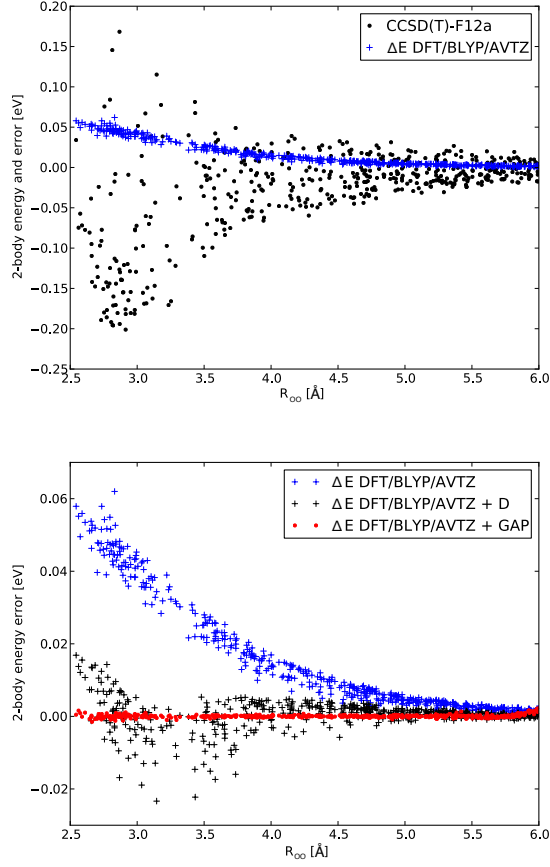


Figure 1: Top: Benchmark 2-body interaction (black) and errors of DFT with BLYP functional (blue) plotted against oxygen-oxygen distance R_{OO} . Benchmarks are computed with CCSD(T) close to the basis-set limit. Bottom: 2-body errors of BLYP (blue, same as in top panel) and errors of BLYP+GAP (red). The RMS deviation of BLYP+GAP from benchmarks is 0.45 meV. Also shown are errors of BLYP plus Grimme D3 dispersion correction [26]. The sample of 500 dimer configurations shown here were drawn from a molecular dynamics simulation of liquid water and not used in the construction of the GAP models.

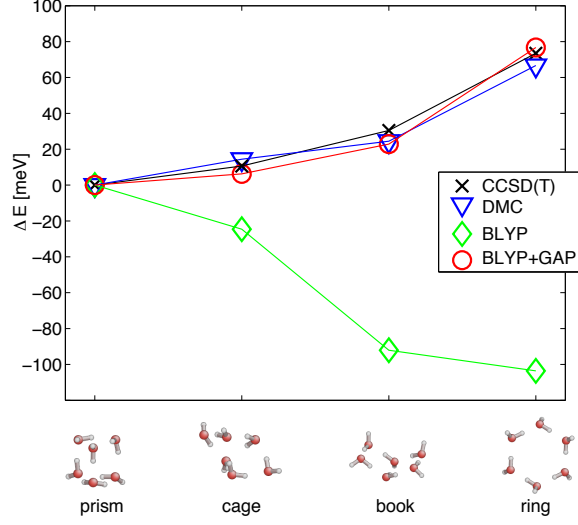


Figure 2: Relative energies (meV units) of four isomers of the water hexamer (atomic coordinates from Ref. [32]) computed with CCSD(T) close to the basis-set limit [7], diffusion Monte Carlo [32], BLYP and BLYP+GAP. Geometries are depicted below the Figure.

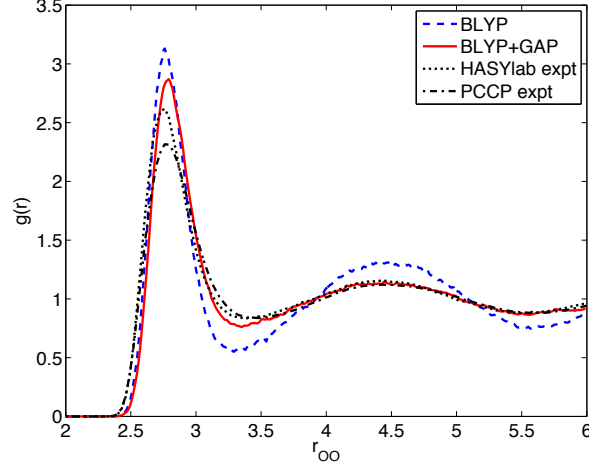


Figure 3: Oxygen-oxygen radial distribution function of liquid water at 308 K at experimental density using BLYP (blue dashed) and BLYP+GAP (red solid) compared with two sets of experimental data (black dotted and dash-dotted). Experimental data are from joint refinement of neutron data and two sets of x-ray data, identified as HASYlab and PCCP (see Ref. [45] for details).

Table 2: Binding energies and volumes of ice polymorphs computing using DFT with the BLYP functional and BLYP+GAP compared with experimental values [45]. Zero-point vibrational contributions have been removed from the experimental energies [49], but not from the volumes.

	Ih	II	VIII	IX	XI	XV
<i>Binding energy</i> [meV]						
BLYP	-540	-458	-318	-475	-544	-403
BLYP+GAP	-667	-672	-637	-670	-671	-657
EXPT	-610	-609	-579	-606		
<i>Binding energy relative to Ih</i> [meV]						
BLYP	0	83	223	66	-3	138
BLYP+GAP	0	-5	30	-3	-4	-11
EXPT	0	1	31	4		
<i>Volume</i> [\AA^3]						
BLYP	31.7	26.0	21.2	28.0	32.1	24.6
BLYP+GAP	30.6	23.8	18.6	24.0	30.6	21.1
EXPT	32.0	25.3	20.1	25.6	32.0	22.9
<i>Volume relative to Ih</i> [\AA^3]						
BLYP	0	-5.7	-10.5	-3.8	0.36	-7.9
BLYP+GAP	0	-6.7	-11.9	-6.5	0	-9.5
EXPT	0	-6.7	-11.9	-6.4	0	-9.2